AIP | Applied Physics Letters

SnTe microcrystals: Surface cleaning of a topological crystalline insulator

M. Saghir, M. Walker, C. F. McConville, and G. Balakrishnan

Citation: Applied Physics Letters **108**, 061602 (2016); doi: 10.1063/1.4941234
View online: http://dx.doi.org/10.1063/1.4941234
View Table of Contents: http://scitation.aip.org/content/aip/journal/apl/108/6?ver=pdfcov
Published by the AIP Publishing

SnTe microcrystals: Surface cleaning of a topological crystalline insulator

M. Saghir,[a] M. Walker, C. F. McConville, and G. Balakrishnan[a]
Department of Physics, University of Warwick, Coventry CV4 7AL, United Kingdom

(Received 30 November 2015; accepted 21 January 2016; published online 8 February 2016)

Investigating nanometer and micron sized materials thought to exhibit topological surface properties that can present a challenge, as clean surfaces are a pre-requisite for band structure measurements when using nano-ARPES or laser-ARPES in ultra-high vacuum. This issue is exacerbated when dealing with nanometer or micron sized materials, which have been prepared *ex-situ* and so have been exposed to atmosphere. We present the findings of an XPS study where various cleaning methods have been employed to reduce the surface contamination and preserve the surface quality for surface sensitive measurements. Microcrystals of the topological crystalline insulator SnTe were grown *ex-situ* and transferred into ultra high vacuum (UHV) before being treated with either atomic hydrogen, argon sputtering, annealing, or a combination of treatments. The samples were also characterised using the scanning electron microscopy, both before and after treatment. It was found that atomic hydrogen cleaning with an anneal cycle (200 °C) gave the best clean surface results. © *2016 AIP Publishing LLC*. [http://dx.doi.org/10.1063/1.4941234]

Since their recent discovery, the study of topological insulators (TIs) has attracted much interest. A new sub-class of these materials called topological crystalline insulators (TCIs) have also been widely studied. In conventional TIs, the degeneracy observed in the band structure is protected by time-reversal symmetry (TRS); however, in TCIs, the role of TRS is replaced by mirror and rotational symmetries.[1–3] A common practice to probe the band structure of TIs and TCIs (such as HgTe, Bi_2Se_3, Bi_2Te_3, and SnTe) is to perform surface sensitive angle-resolved photoemission spectroscopy (ARPES) measurements.[4–6] Samples are usually bulk crystals that have been cleaved inside the vacuum chamber or thin films that have grown *in-situ*.

The weak signal arising from the exotic surface properties of TIs and TCIs is thought to be difficult to detect. To combat this, there has been a focus to increase the surface area to volume ratio (SAVR) of such materials hoping that the exotic surface properties become more readily observable.[7] There have been numerous successful examples for the conversion of TIs and TCIs from bulk to nanoform using a variety of growth techniques, including both wet and dry synthesis methods.[8–14] In this letter, we demonstrate effective cleaning methods in ultra high vacuum (UHV) of high SAVR materials, which have been exposed to atmosphere. With this information, we explore a preparation method that can negate the effects of surface contamination and allow the more exotic surface states of the TCIs to be explored.

The IV-VI semi-metal SnTe is a TCI, which forms in a cubic rock-salt structure (lattice constant, $a = 0.63$ nm). It was the first material thought to exhibit TCI behaviour, which was later confirmed by ARPES measurements revealing Dirac cone surface states.[6] Starting from bulk crystals of SnTe, microcrystals were grown using a vapour-liquid-solid growth process as described in our previous work[15] and by others.[13,14] Samples were then transferred through atmosphere and placed into an XPS system (details described below). The levels of surface contamination were investigated using XPS, while SEM was used to characterise the surface topography both before and after cleaning. We found that the optimum treatment to remove the adsorbed oxygen and adventitious carbon was to perform atomic hydrogen cleaning at elevated temperature which both cleaned the surface and retained its topography. Sputtering the surface with argon was also investigated; however, it was not found to be as effective as atomic hydrogen in removing surface contamination. In addition, the sputtering process also caused a significant degree of damage to the microcrystal surface, while removing surface impurities with just annealing cycles in UHV proved to be ineffective.

The samples investigated in this study were mounted on Omicron sample plates using tantalum foil and loaded into the fast-entry chamber. Once a pressure of $<1 \times 10^{-7}$ mbar had been achieved (approx. 1 h), the samples were transferred to a 12-stage storage carousel, located between the preparation and main analysis chambers, for storage at pressures of less than 2×10^{-10} mbar.

XPS measurements were conducted at room temperature in the main analysis chamber (base pressure 2×10^{-11} mbar), with the sample being illuminated using a monochromatic Al $K\alpha_1$ x-ray source (Omicron Nanotechnology GmbH). The photoelectrons were detected at normal emission using a Sphera hemispherical electron analyser (Omicron Nanotechnology), with the core levels recorded using a pass energy of 10 eV (resolution approx. 0.47 eV). These data were analysed using the CasaXPS package, using a combination of Shirley background subtraction, mixed Gaussian-Lorentzian (Voigt) lineshapes, and asymmetry fitting parameters where appropriate. All binding energies were calibrated using the Fermi edge of a polycrystalline Ag sample, measured immediately prior to commencing the measurements.

In-situ sample preparation was conducted with a variety of instruments attached to the vacuum system. Ion bombardment was conducted in the analysis chamber at room temperature using an incident beam of 500 eV Ar^+ ions, generated

[a]M.Saghir@warwick.ac.uk and G.Balakrishnan@warwick.ac.uk

using a low energy ion gun (FIG 05, Physical Electronics Inc, USA). Atomic hydrogen exposure was facilitated by a thermal gas cracker source (TC-50 Oxford Applied Research, UK) in the preparation chamber, with an estimated H_2 cracking efficiency of 50%–60%.[16] All atomic hydrogen doses were conducted over a 15 min duration using a pressure of 1×10^{-6} mbar (675 L total per dose [H* and H_2 combined]), with the sample held at the chosen temperature for the duration of H dosing and for a subsequent 5 min in the absence of the H flow. Sample annealing was achieved using a radiative heater located on the manipulators in both the preparation and analysis chambers, with the sample temperature measured using a pre-calibrated chromel-alumel thermocouple.

In total, four different treatment methods were investigated and each treatment was conducted on a fresh sample. These included: (i) argon sputtering at room temperature, (ii) atomic hydrogen cleaning at room temperature, (iii) atomic hydrogen cleaning at elevated temperatures, and (iv) just annealing in UHV. SEM was used to compare the effects of the more effective cleaning methods on the surface morphology. Energy dispersive x ray (EDX) measurements were performed in order to compare the surface and bulk stoichiometries with XPS results. XPS chemical shifts also provided an insight in the different oxides formed at the surface during exposure to atmosphere.

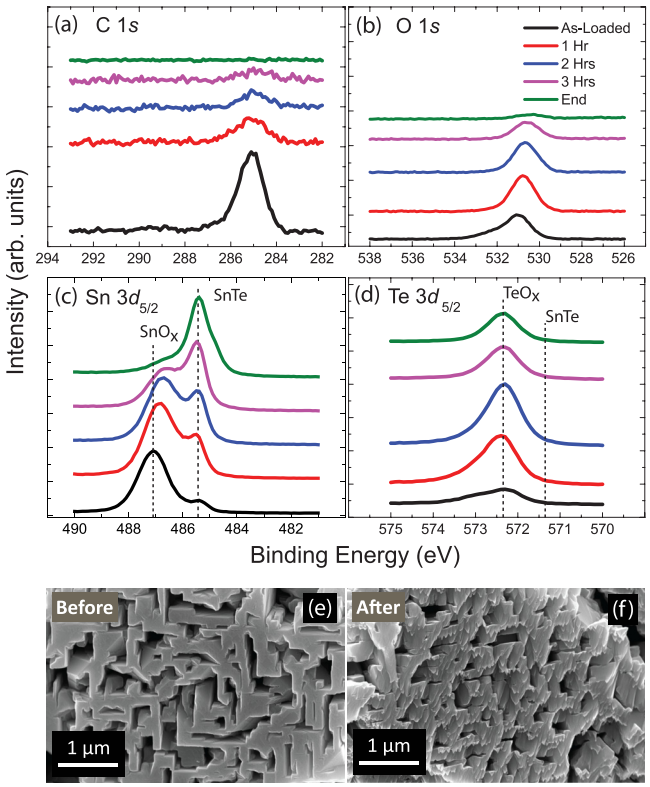

FIG. 1. XPS spectra for the (a) C1 s, (b) O 1s, (c) Sn $3d_{5/2}$, and (d) Te $3d_{5/2}$ core-level peaks following multiple argon sputtering cycles at room temperature. The data presented show chemical shifts for an as-loaded sample (black), the effects after 1 h (red), 2 h (blue), 3 h (purple), and the end of the treatment cycle (green). SEM images (e) and (f) show how the treatment affects the morphology of the sample surface. Damage to the surface can be clearly seen in the form of "shadow cones" formed, the direction of which are dependent on the incident direction of the argon ions.

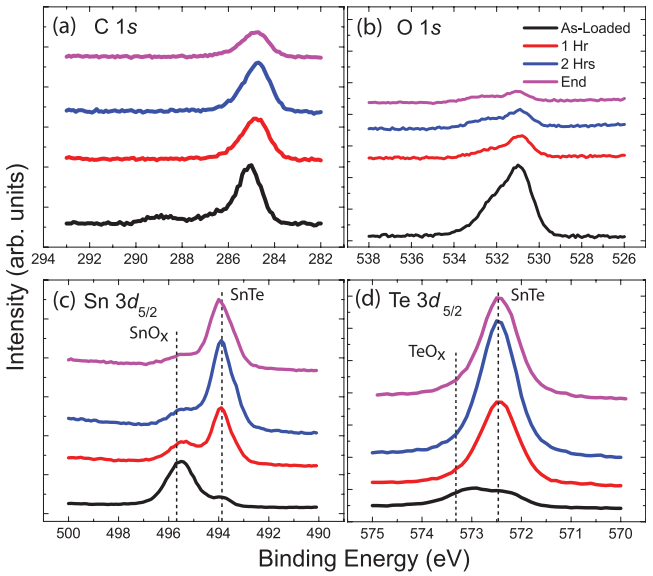

FIG. 2. XPS spectra for the (a) C 1s, (b) O 1s, (c) Sn $3d_{5/2}$, and (d) Te $3d_{5/2}$ core-level peaks. Samples were subject to an atomic hydrogen cleaning cycle at room temperature, and the data presented show the chemical shifts for an as-loaded sample (black), the effects after 1 h (red), 2 h (blue), and the end of the treatment cycle (purple).

Figures 1–4 show the effectiveness of removing the oxide layer and the adventitious carbon formed at the surface for the four different cleaning methods. They also show the changes to the Sn $3d_{5/2}$ and Te $3d_{5/2}$ peaks as a result of various treatments. The Sn $3d_{5/2}$ peak was fit with two components for SnTe and SnO_2 with the positions at a binding

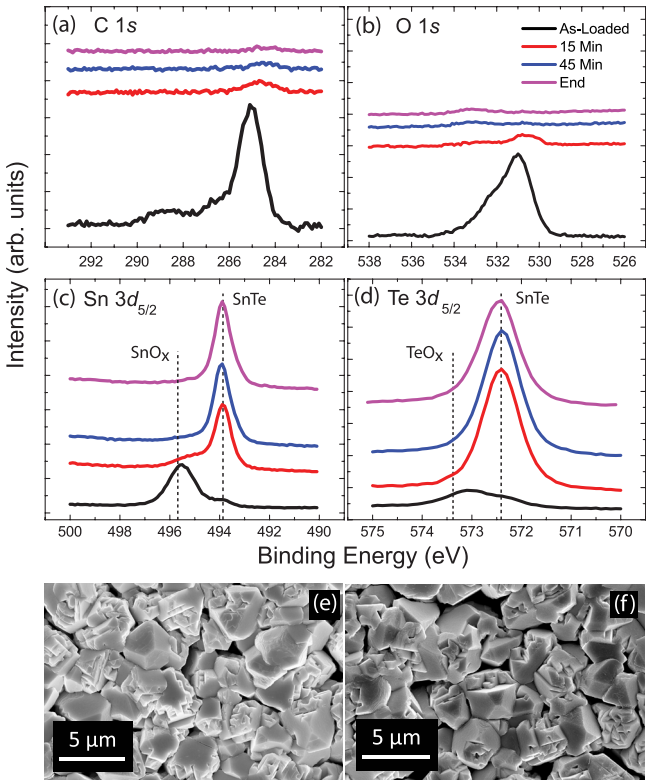

FIG. 3. XPS spectra for the (a) C 1s, (b) O 1s, (c) Sn $3d_{5/2}$, and (d) Te $3d_{5/2}$ core-level peaks. Samples were subject to an atomic hydrogen cleaning cycle at 200 °C, and the data presented show the chemical shifts for an as-loaded sample (black), the effects after 1 h (red), 2 h (blue), and the end of the treatment cycle (purple). (e) and (f) SEM images of microcrystals pre- and post-treatment showing no change to the surface morphology.

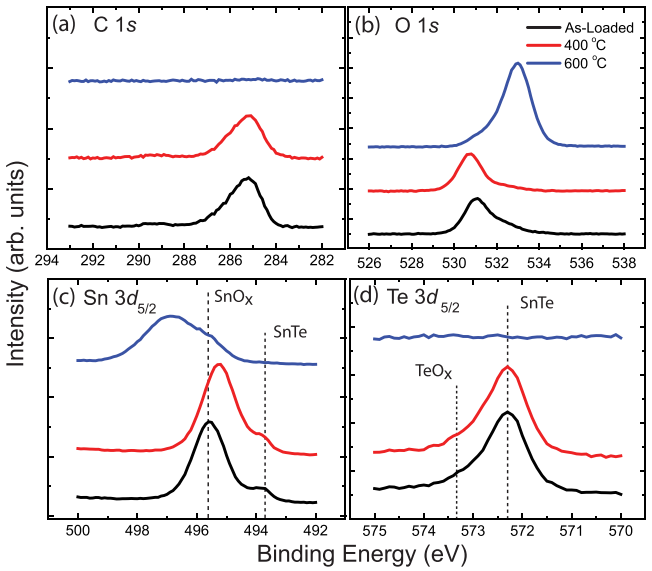

FIG. 4. XPS spectra for the (a) C 1s, (b) O 1s, (c) Sn $3d_{5/2}$, and (d) Te $3d_{5/2}$ core-level peaks following annealing at 200 °C (red) and 600 °C (blue). The data presented show chemical shifts for an as-loaded sample (black). A significant reduction in Te at the surface can be seen, further confirming the change in surface stoichiometry observed at elevated temperatures.

energy (B.E.) of 485.4 ± 0.1 eV and 487.1 ± 0.1 eV, respectively. The value for the B.E. of SnO_2 is consistent with that reported in reference tables and literature.[17] The full width at half maximum and the energy difference of the two components were constrained during fitting. Five components were used to fit the Te $3d_{5/2}$ peak, three of which were attributed to the two possible oxidation methods and intermediate oxide phases for the formation of TeO_2. The B.E. for SnTe and Te^{4+} were found to be 572.3 ± 0.1 eV and 576.8 ± 0.1 eV, respectively. A summary of the binding energies can be found in Table I.

Figures 1 and 2 show that at room temperature, both argon sputtering and atomic hydrogen cleaning were similar in effectiveness. While both reduced the intensity of the C1s present at the surface, there was still a noticeable peak showing the presence of the oxide with argon sputtering after 4 h. Figure 1 also shows that the Sn and Te peaks are still quite broad, owing to the presence of SnO_x and TeO_x at the surface, compared to those observed in Figure 2, for atomic hydrogen cleaning at room temperature. SEM revealed that the surface morphology had changed with the introduction of "shadow cones" to the surface after ion bombardment. Such features can be seen in Figure 1(f). EDX showed no change in the bulk stoichiometry after room temperature treatments with argon sputtering or atomic hydrogen treatment. The stoichiometry at the surface determined from XPS also remained the same post-treatment for both argon sputtering and atomic hydrogen cleaning, and furthermore, it appears to be Sn-rich, suggesting the majority of the surface oxide is SnO_x (see Table II).

TABLE I. The B.E. for the fitted components of Sn $3d_{5/2}$ and Te $3d_{5/2}$ peaks.

Component	B.E. (eV)
Sn^{2+}	485.4 (±0.1)
Sn^{4+}	487.1 (±0.1)
Te^{2-}	572.3 (±0.1)
Te^{4+}	576.8 (±0.1)

TABLE II. Representative atomic compositions for the bulk and the surface of SnTe microcrystals obtained using EDX and XPS analysis (within an error of 2% concentration).

Treatment	EDX	XPS
Argon sputtering	$Sn_{49(2)}Te_{51(2)}$	$Sn_{60(2)}Te_{39(0)}$
AHC	$Sn_{48(2)}Te_{52(2)}$	$Sn_{64(2)}Te_{35(2)}$
AHC + 200 °C	$Sn_{49(2)}Te_{51(2)}$	$Sn_{54(2)}Te_{45(2)}$

In order for the cleaning to yield a smooth surface as seen in Figure 1(e), an anneal cycle was introduced following argon sputtering. Annealing at temperatures of up to 600 °C was investigated along with dose lengths up to 24 h. XPS revealed that for temperatures >300 °C, large amounts of Te evaporated from the surface destroying the surface stoichiometry. However, it was found that annealing at 200 °C preserved the stoichiometry of the surface which was further confirmed by both EDX and XPS measurements. However, the "shadow cones" present due to sputtering were not removed after either anneal cycle.

Figure 3 shows XPS data for samples exposed to atomic hydrogen at 200 °C. This method was found to be most effective for several reasons. First, heating the sample to 200 °C allowed for the removal of the surface oxides and the carbon peaks to a greater extent than those observed for argon sputtering and atomic hydrogen cleaning at room temperature. A subsequent XPS analysis revealed a change in the surface stoichiometry with the Sn:Te ratio approaching that observed in the bulk with EDX. Second, the time required to clean the surface of the sample reduced vastly compared to ion bombardment and annealing, with the residual surface oxides and carbon components reaching near background levels after ≈1 h. Third, the morphology of the sample surface remained the same after treatment, as can be seen in Figure 3(f). Finally, compositional analysis of the bulk of the microcrystals with EDX analysis post-treatment showed no change in the stoichiometry. Similar results were observed for the surface stoichiometry from XPS and can be found in Table II.

Figure 4 shows XPS data for samples just annealed at 200 °C and 600 °C in UHV conditions. These data show that just an anneal cycle in UHV was ineffective in removing surface contamination. It further confirms the loss of Te that occurs at elevated temperatures. This was observed when attempting to restore the smooth nature of the surface after argon sputtering.

With regard to the exposure or dose, it is clear that atomic hydrogen cleaning at 200 °C offered the most promising route to a surface, which would be sufficiently clean to conduct surface sensitive measurements such as ARPES. It is worth noting that due to the geometry of the sample and sputter gun, it was not possible to remove the oxide and carbon from the edges of the microcrystals; however, the surface normal to the substrate had been successfully cleaned and restored without a stoichiometric change in the bulk and surface of the sample. This limitation was overcome for atomic hydrogen cleaning as the gas cracker could be aligned with the surface normal.

In this study, the most effective methods for preparing the surface of microcrystals of the topological crystalline insulator, SnTe, have been investigated. It was found that cleaning with thermally cracked atomic hydrogen for a minimum of 15 min at 200 °C removed sufficient amounts of surface oxide and carbon to perform measurements such as ARPES. By performing SEM on pre- and post-treated samples, it was found that damage did not occur to the surface of the material with atomic hydrogen cleaning, whereas Ar^+ sputtering gave rise to the formation of "shadow cones." This optimal cleaning procedure was also able to restore the bulk stoichiometry at the sample surface, as evidenced by the comparison of EDX and XPS measurements. The data presented describe an effective pathway to obtain clean surfaces of materials with exotic topologically protected states for surface sensitive measurements.

This work was supported by the EPSRC, UK (EP/L014963/1). Some of the equipment used in this research was obtained through the Science City Research Alliance (SCRA) Advanced Materials Project 1: Creating and Characterizing Next Generation Advanced Materials Project, with support from Advantage West Midlands (AWM), and was partially funded by the European Regional Development Fund (ERDF). The x-ray photoemission spectroscopy (XPS) data were collected at the University of Warwick Photoemission Facility. The authors thank T. E. Orton and R. Johnston for valuable technical support.

[1]D. Hsieh, D. Qian, L. Wray, Y. Xia, Y. S. Hor, R. J. Cava, and M. Z. Hasan, Nature **452**, 970 (2008).
[2]D. Hsieh, Y. Xia, L. Wray, D. Qian, A. Pal, J. H. Dil, J. Osterwalder, F. Meier, G. Bihlmayer, C. L. Kane, Y. S. Hor, R. J. Cava, and M. Z. Hasan, Science **323**, 919 (2009).
[3]Y. Xia, D. Qian, D. Hsieh, L. Wray, A. Pal, H. Lin, A. Bansil, D. Grauer, Y. S. Hor, R. J. Cava, and M. Z. Hasan, Nat. Phys. **5**, 398 (2009).
[4]M. Z. Hasan and C. L. Kane, Rev. Mod. Phys. **82**, 3045 (2010).
[5]W. Zhang, Y. Cheng, J. Hu, J. Zhan, W. Yu, L. Yang, and Y. Qian, Chem. Lett. **29**, 446 (2000).
[6]T. H. Hsieh, H. Lin, J. Liu, W. Duan, A. Bansil, and L. Fu, Nat. Commun. **3**, 982 (2012).
[7]J. J. Cha, J. R. Williams, D. Kong, S. Meister, H. Peng, A. J. Bestwick, P. Gallagher, D. Goldhaber-Gordon, and Y. Cui, Nano Lett. **10**, 1076 (2010).
[8]D. Kong, J. C. Randel, H. Peng, J. J. Cha, S. Meister, K. Lai, Y. Chen, Z. X. Shen, H. C. Manoharan, and Y. Cui, Nano Lett. **10**, 329 (2010).
[9]Z. Wang, R. L. J. Qiu, C. H. Lee, Z. Zhang, and X. P. A. Gao, ACS Nano **7**, 2126 (2013).
[10]P. Gehring, B. F. Gao, M. Burghard, and K. Kern, Nano Lett. **12**, 5137 (2012).
[11]P. Yang, H. Yan, S. Mao, R. Russo, J. Johnson, R. Saykally, N. Morris, J. Pham, R. He, and H.-J. Choi, Adv. Funct. Mater. **12**, 323 (2002).
[12]Q. Wei, Y. Su, C. J. Yang, Z. G. Liu, H. N. Xu, Y. D. Xia, and J. Yin, J. Mater. Sci. **46**, 2267 (2010).
[13]Z. Li, S. Shao, N. Li, K. McCall, J. Wang, and S. X. Zhang, Nano Lett. **13**, 5443 (2013).
[14]M. Safdar, Q. Wang, M. Mirza, Z. Wang, K. Xu, and J. He, Nano Lett. **13**, 5344 (2013).
[15]M. Saghir, M. R. Lees, S. J. York, and G. Balakrishnan, Cryst. Growth Des. **14**, 2009 (2014).
[16]M. Draxler, M. Walker, and C. F. McConville, Nucl. Instrum. Meth. B **249**, 886 (2006).
[17]V. Neudachina, T. Shatalova, V. Shtanov, L. Yashina, T. Zyubina, M. Tamm, and S. Kobeleva, Surf. Sci. **584**, 77 (2005).